Functional characterization of CDK10 and cyclin M truncated variants causing severe developmental disorders

Thomas Robert, Anne-catherine Dock-bregeon, Pierre Colas

Molecular Genetics & Genomic Medicine
Open Access WILEY

Functional characterization of CDK10 and cyclin M truncated variants causing severe developmental disorders

Thomas Robert | Anne-Catherine Dock-Bregeon | Pierre Colas 🟢

Laboratory of Integrative Biology of Marine Models, Station Biologique de Roscoff, Sorbonne Université/CNRS, Roscoff, France

Correspondance
Pierre Colas, Laboratory of Integrative Biology of Marine Models, Station Biologique, Place Georges Teissier, 29680 Roscoff, France.
Email: colas@sb-roscoff.fr

Abstract

Background: CDK10 is a poorly known cyclin M (CycM)-dependent kinase. Loss-of-function mutations in the genes encoding CycM or CDK10 cause, respectively, STAR or Al Kaissi syndromes, which present a constellation of malformations and dysfunctions. Most reported mutations abolish gene expression, but two mutations found in 3' exons could allow the expression of CDK10 and CycM truncated variants.

Methods: We built a structural model that predicted a preserved ability of both variants to form a CDK10/CycM heterodimer. Hence, we functionally characterized these two truncated variants by determining their capacity to heterodimerize and form an active protein kinase when expressed in insect cells, by examining their two-hybrid interaction profiles when expressed in yeast, and by observing their expression level and stability when expressed in human cells.

Results: Both truncated variants retain their ability to form a CDK10/CycM heterodimer. While the CycM variant partially activates CDK10 activity *in vitro*, the CDK10 variant remains surprisingly inactive. Expression in human cells revealed that the CDK10 and CycM variants are strongly and partially degraded by the proteasome, respectively.

Conclusion: Our results point to a total loss of CDK10/CycM activity in the Al Kaissi patient and a partial loss in the STAR patients.

KEYWORDS
Al Kaissi syndrome, CDK10, cyclin M, interaction profiling, protein kinase, STAR syndrome

1 | INTRODUCTION

Although discovered in the pre-genomic era and despite recent significant advances, CDK10 remains one of the most elusive members of the cyclin-dependent kinase family (Guen, Gamble, Lees, & Colas, 2017). It interacts with cyclin M (CycM) to form an active protein kinase that

phosphorylates and controls the stability of the ETS2 oncoprotein (Guen et al., 2013). CDK10/CycM also takes part in the control of actin network architecture and ciliogenesis through a PKN2-RhoA regulatory pathway (Guen et al., 2016). Loss-of-function mutations in *CCNQ* (formerly *FAM58A*, OMIM # 300708), the gene-encoding CycM, cause an X-linked dominant developmental disorder

dubbed STAR syndrome that entails toe syndactyly, telecanthus, anogenital and renal malformations, and additional sporadic defects, including heart, eyes, cranial bone anomalies (Unger et al., 2008), reviewed in Colas (2020). Autosomal recessive loss-of-function mutations in *CDK10* (OMIM # 603464) cause another developmental disorder (dubbed Al Kaissi syndrome) that includes growth retardation, spine malformation, facial dysmorphisms and intellectual disability (Windpassinger et al., 2017). In congruence with CDK10/CycM gene silencing experiments in human cell lines, enhanced ETS2 protein levels were detected in cells derived from STAR (Guen et al., 2013) and Al Kaissi (Windpassinger et al., 2017) syndrome patients, and abnormal, elongated cilia were detected in a STAR patient renal biopsy (Guen et al., 2016).

Among the very few reported cases of both syndromes (12 STAR, 10 Al Kaissi), four patients present two mutations that stand out from all others in that they may allow the expression of a C-terminally truncated form of either CDK10 or CycM. A young girl, her mother and the maternal half-sister were diagnosed with STAR syndrome, presenting the cardinal above-mentioned features and expanded phenotypes including tethered cord (all three individuals), sacral dimple and hemangioma (both half-sisters), hearing loss (proband). Whole-exome sequencing revealed the first and only *CCNQ* non-sense variant identified so far (Boczek et al., 2017). Because it is located in the last exon of the gene, the mutation (NM_152274:c.651G>A, p.(Trp217X)) is unlikely to trigger non-sense-mediated decay (NMD) of the mRNA (Kurosaki, Popp, & Maquat, 2019), and it may allow the translation of a CycM variant devoid of its last 32 carboxy-terminal amino acids. Besides the identification of a cohort of nine Al Kaissi syndrome patients (Windpassinger et al., 2017), a young girl presenting a homozygous dinucleotide deletion in the 11th of the 13 exons of *CDK10* (NM_052988.4:c.870_871del, p.(Trp291Alafs*18)) was reported. In addition to the growth delay, facial and skeletal anomalies and cognitive deficits observed in the cohort, this patient suffered from heart failure, vocal cord paralysis, bilateral deafness and retina pigmentosis (Guen et al., 2018). Whereas the study of the nine patients from the cohort revealed NMD of mutant transcripts (Windpassinger et al., 2017), the study of the young girl showed that the mutant transcript was not degraded but even slightly more abundant, potentially allowing the translation of a shorter CDK10 protein (307 amino acids vs. 360 for the longest wild-type isoform), with 17 missense amino acids and without the bipartite nuclear localization sequence located at its carboxy terminus (Guen et al., 2018).

Here, we functionally characterize this CDK10 and this CycM variant by determining their capacity to heterodimerize and form an active protein kinase when expressed in insect cells, by examining their two-hybrid interaction profiles when expressed in yeast, and by observing their expression level and stability when expressed in human cells.

2 | MATERIALS AND METHODS

This study did not call for an ethics committee approval.

2.1 | Structural modelling of the CDK10/CycM heterodimer

Phyre2 revealed high-confidence structural alignments between CDK10 and several kinases, among which was CDK12 in complex with CycK (PDB ID: 4NST, confidence score: 100%, sequence identity: 43%) and CDK9 in complex with CycT (PDB ID: 3MI9, confidence score: 100%, sequence identity: 41%). We chose CDK12 as a template as it contains fewer insertions or deletions. CDK10 residues 32-343 were modelled, which represents an 86% coverage. The best Phyre2 hit for CycM was obtained with the crystal structure of free CycK (PDB ID: 2I53, confidence score: 100%, sequence identity: 27%). CycM residues 19-246 were modelled, which represents a 91% coverage. We delineated the binding interface with COCOMAPS (Vangone, Spinelli, Scarano, Cavallo, & Oliva, 2011).

2.2 | Plasmid constructions

Constructions were performed using the GenBank reference sequences NM_052988.3 and NM_152274.5 for *CDK10* and *CNNQ*, respectively.

2.2.1 | Insect cell expression plasmids

We performed site-directed mutagenesis of pFast-BacDual:GST-WT CDK10/Strep2-WT CycM (Robert et al., 2020) using a Quickchange kit (Agilent). For the p.(Trp291Alafs*18) CDK10 variant, we used the oligonucleotides 5′-GAAGCACAAGTTCCCGGCTGTCGGAGGCCG-3′ and 5′-CGGCCTCCGACAGCCGGGAACTTGTGCTTC-3′, which deleted nucleotides 870-871 in the coding sequence. Our CDK10 WT coding sequence contains a silent C894T nucleotide substitution, which is no longer silent after the frameshift caused by this double deletion. We thus corrected this mutation using the oligonucleotides 5′-GGCCGGGCTGCGCCTGCTGCACTTC-3′ and 5′-GAAGTGCAGCAGGCGCAGCCCGGCC-3′. For the p.(Trp217X) CycM variant, we used the oligonucleotides

5′-GCTGAGAAGCCGTGATGGCAGGTGTTTAATGAC-3′ and 5′-GTCATTAAACACCTGCCATCACGGCTTCTCAGC-3′ that introduced a stop codon at Trp217.

2.2.2 | Mammalian cell expression plasmids

We digested pCMV-Tag3B:WT CDK10 (a plasmid that directs the expression of Myc-tagged WT CDK10, Guen et al., 2013) and pJG4-5:p.(Trp291Alafs*18) CDK10 (see below) with EcoRI and XhoI. We ligated the insert of the latter digestion into the plasmid of the former digestion to obtain pCMV-Tag3B:p.(Trp291Alafs*18) CDK10. We digested pFlag:ETS2 (a plasmid that directs the expression of Flag-tagged ETS2, Guen et al., 2013) and pEG202:WT and p.(Trp217X) CycM with EcoRI and XhoI. We ligated the inserts of the latter digestions into the plasmid of the former digestion to obtain pFlag:WT CycM and pFlag:p.(Trp217X) CycM.

2.2.3 | Yeast two-hybrid plasmids

Constructions of WT CDK10, WT CycM, ETS2 bait and prey plasmids were described in Guen et al. (2013). We amplified the p.(Trp291Alafs*18) CDK10 coding sequence from pFastBacDual:GST-p.(Trp291Alafs*18) CDK10/Strep2-WT CycM using the oligonucleotides 5′-ATATGAATTCATGGCGGAGCCAGATCTGGAG-3′ and 5′-ATATCTCGAGTCAG GGTTTACAGCGCTTGC-3′ that contain an EcoRI and an XhoI site, respectively. We ligated the PCR product into EcoRI/XhoI-cut pEG202 and pJG4-5 to construct the p.(Trp291Alafs*18) CDK10 bait and prey plasmids, respectively. We used the same procedure to construct the p.(Trp217X) CycM bait and prey plasmids using pFastBacDual:GST-WT CDK10/Strep2-p.(Trp217X) CycM and the oligonucleotides 5′-ATATGAATTCATGGAAGCCCCGGAGGGCGGC-3′ and 5′-ATATCTCGAGTTAGGGGATCTCTGTGTCCATGG-3′. To remove the NLS from pEG202:WT CDK10, we performed site-directed mutagenesis using a Quickchange XL kit (Agilent) and the oligonucleotides 5′-CCTCCGAGGGCCAGAGCGCGGCCTGTAAACCCTGACTCG-3′ and 5′-CGAGTCAGGGTTTACAGGCCGCGCTCTGGCCCTCGGAGG-3′, which produced a double mutation Lys356Ala/Arg357Ala (Sergere, Thuret, Le Roux, Carosella, & Leteurtre, 2000). We amplified the SALL1 coding sequence from pDEST:SALL1 (Source BioScience) using the oligonucleotides 5′-ATATGAATTCTCAGCAGCGAAGCAAGCGAAGCCTCAACATTTCC-3′ and 5′-ATATGTCGACTTAACTCGTGACGATCTCCTTGC-3′ that contain an EcoRI and a SalI site, respectively. The former oligonucleotide produces a double mutation Arg3Ala/Arg4Ala in order to abolish the transcriptional repressor activity of SALL1 (Lauberth & Rauchman, 2006). We ligated the PCR product into EcoRI/XhoI-cut pEG202 and pJG4-5.

2.3 | Protein expression and purification, protein kinase assay, Western blots on recombinant proteins

We expressed and purified the GST-CDK10/Strep2-CycM heterodimers in insect cells, and we performed *in vitro* protein kinase assays as recently described (Robert et al., 2020). We loaded equal amounts of heterodimers onto NuPage MOPS 12% polyacrylamide gel, transferred onto a nitrocellulose membrane and probed the upper and lower half of the membrane with an anti-GST (1/3000; Abcam 19256) and an anti-Strep2 (1/1250; Abcam 76949) antibody, respectively. We revealed the blots with an HRP-coupled swine anti-rabbit antibody (1/5000; DAKO P0217) and an ECL detection kit (GE Healthcare 34095).

2.4 | Yeast two-hybrid assays

We used yeast two-hybrid interaction trap mating assays (Finley & Brent, 1994). We transformed *S. cerevisiae* EGY42a (*leu2*, *ADE2*, *trp1*, *ura3*, *his3*) with prey plasmids, and we co-transformed TB50α (*leu2*, *ADE2*, *trp1*, *ura3*, *his3*) with bait plasmids and pSH18-34T, a high-sensitivity *lacZ* reporter plasmid, using a standard LiAc/single-strand carrier DNA/PEG method (Gietz & Woods, 2006). We resuspended transformants in sterile water and allowed them to mate by spotting 3 μl of suspensions onto a rich solid medium in a matrix format. Twenty-four hours later, we streaked the spots onto SD-UHW solid medium to select for diploids. Twenty-four hours later, we resuspended the diploids in 20 μl sterile water in a 96 round-bottom multi-well plate. We spotted 5 μl of yeast suspensions onto SD-UHW + X-Gal and SGR-UHW + X-Gal plates using a multi-channel pipette, and we incubated the plates for 48 h at 30°C.

2.5 | Human cell expression experiments and Western blots

We cultured hTERT-RPE1 cells in DMEM/F12 Glutamax medium with 10% foetal bovine serum (Life Technologies). We grew the cells in six well-plates to reach an 80% confluence, transfected them with 2.5 μg expression plasmids using lipofectamine 3000 (Invitrogen L3000-008), collected and lysed them 48 h after transfection using the

M-PER mammalian protein extraction reagent (Thermo 78503). We added MG132 (final concentration 10 μM, 0.1% DMSO) 16 h prior to cell lysis. We loaded equal amounts of protein extracts onto NuPage MOPS 4–12% polyacrylamide gels, transferred them onto nitrocellulose membranes and probed the upper halves of the membranes with an anti-tubulin monoclonal antibody (1/5000, Sigma B512). We probed the lower halves with either an anti-Myc monoclonal antibody (1/1000, Cell signalling 9B11) or an anti-Flag antibody (1/700, Sigma 7425). We revealed the Flag blots with the same antibody as described above and a SuperSignal West Femto ECL kit (Thermo 34095). We revealed the Myc and the tubulin blots with an HRP-coupled goat anti-mouse antibody (1/1500, DAKO P0447) and the SuperSignal or the regular ECL detection kit, respectively.

3 | RESULTS

3.1 | Structural model of the CDK10/CycM heterodimer

In order to predict the structural consequences of the C-terminal truncations of the CDK10 and CycM mutant forms, we built a model of the CDK10/CycM heterodimer. Using the Phyre2 web server (Kelley, Mezulis, Yates, Wass, & Sternberg, 2015), we first obtained a CycM model from an alignment with the crystal structure of CycK, and a CDK10 model from the crystal structure of CDK12 in complex with CycK. We then built a model for the CDK10/CycM heterodimer using PyMOL, replacing the CycK moiety with the CycM model. The binding interface involves the N-terminal domain of CDK10 and comprises, as seen in other CDKs, the first helix α1 (residues 79–92, containing the PISSLRE motif) and the loop β4–β5 (residues 105–112). On the CycM side, the interface comprises

residues of helix α3 and a large half of helix α5 (Figure 1a). Although we cannot exclude that the heterodimer interface involves additional elements, this model strongly suggests that the C-terminal truncations and modifications exhibited by the two truncated variants should not prevent the formation of the CDK10–CycM complex (Figure 1b).

3.2 | Protein interaction and protein kinase assays

To test this prediction, we co-expressed GST-p.(Trp291Alafs*18) CDK10 and Str-WT CycM on the one hand and GST-WT CDK10 and Str-p.(Trp217X) CycM on the other hand, using an insect cell dual expression system that recently allowed us to identify small-molecule inhibitors of the CDK10/CycM protein kinase (Robert et al., 2020). We submitted the insect cell lysates containing these protein combinations to glutathione-sepharose affinity chromatography, in addition to GST-WT CDK10/Str-WT CycM and GST-KD CDK10/Str-WT CycM (the kinase-dead CDK10 mutant) as controls. We observed that the level of expression of GST-p.(Trp291Alafs*18) CDK10 was lower than that of GST-WT CDK10 and GST-KD CDK10 (not shown). We thus adjusted cell lysate amounts to aim at comparable input levels of GST-CDK10 proteins, which were equally captured and eluted from the glutathione matrix (Figure 2a, upper panel). Str-WT CycM co-purified with GST-p.(Trp291Alafs*18) CDK10 nearly as much as it did with GST-WT CDK10, and Str-p.(Trp217X) CycM co-purified with GST-WT CDK10 nearly as much as Str-WT CycM (Figure 2a, lower panel). These results confirm the prediction of the structural model and establish that the C-terminal truncations and modifications caused by the two CDK10 and CycM pathogenic mutations preserve the formation of CDK10/CycM heterodimers, with no detectable loss of apparent affinity.
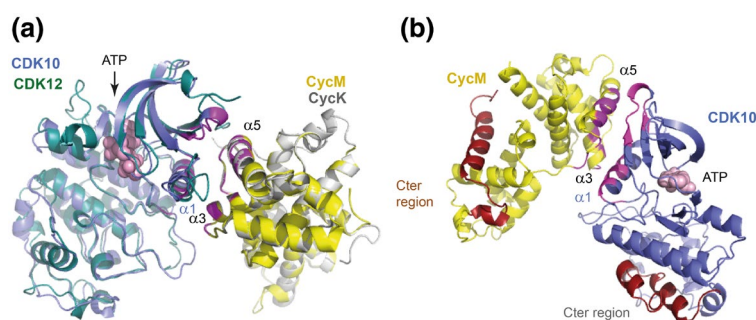

FIGURE 1 Structural model of the CDK10/CycM heterodimer. (a) Superposition of CDK10 (blue)/CycM (yellow) on the crystal structure of CDK12 (dark green)/CycK (grey). The CDK–cyclin binding interface is coloured in magenta, and the involved helices are labelled. The ATP molecule observed in CDK12 is shown with pink spheres, located between the N- and C-terminal domains of CDK12. (b) 180° rotation of the view presented in (a), showing the C-terminal regions of CDK10 and CycM (dark red) that are truncated in the two pathogenic variants analysed herein
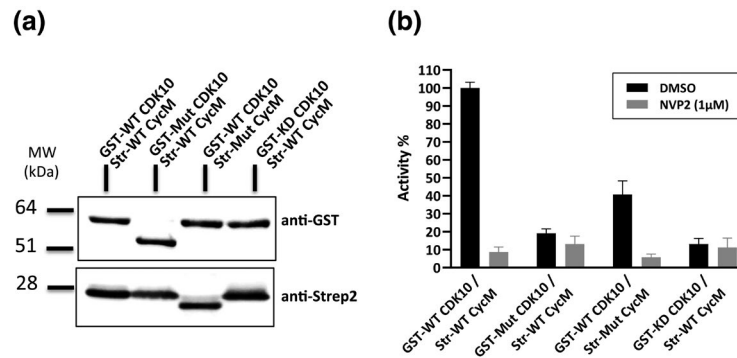
FIGURE 2 CDK10/CycM heterodimerization and kinase assays. (a) Co-purification of GST-CDK10/Str-CycM proteins from insect cell lysates loaded onto a glutathione-sepharose matrix. Upper panel: Western blot using an anti-GST antibody, revealing the capture of GST-CDK10 fusion proteins; lower panel: Western blot using an anti-Strep2 tag antibody, revealing the co-capture of Str-CycM fusion proteins. (b) *In vitro* CDK10/CycM protein kinase assays. Luminescence values were normalized with those of the WT CDK10/WT CycM kinase. Assays were performed in sextuplets. All differences in kinase activity are statistically significant (Mann-Whitney test, $p < .01$) except for the differences between p.(Trp291Alafs*18) and KD CDK10 and the differences between p.(Trp291Alafs*18) CDK10 with and without the NVP-2 inhibitor. 'Mut CDK10' and 'Mut CycM' designate p.(Trp291Alafs18*) CDK10 and p.(Trp217X) CycM, respectively
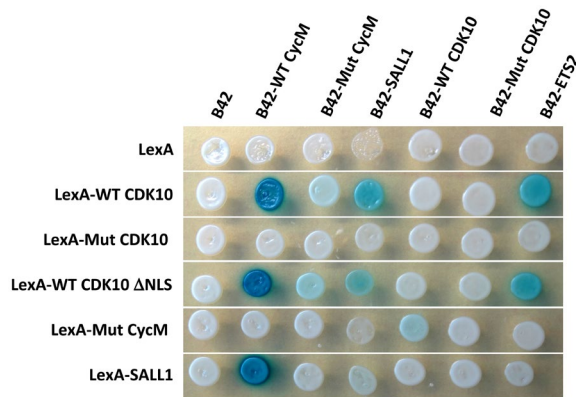

FIGURE 3 Yeast two-hybrid protein interaction profiling. Bait proteins (horizontal lines) are expressed in fusion with the LexA DNA-binding domain and prey proteins (vertical lines) are expressed in fusion with the B42 transcription activation domain. The *lacZ* reporter gene is transcribed upon an interaction between bait and prey, which produces a blue colour on an X-gal-containing medium. For a given bait, the intensity of the blue colour is indicative of the strength of its interactions with preys. To rule out that the undetectable interaction phenotype between LexA-p.(Trp291Alafs*18) CDK10 (LexA-Mut CDK10 in the figure) and B42-WT CycM might be due to the absence of the NLS located at the C-terminus of WT CDK10, we performed site-directed mutagenesis of pEG:WT-CDK10 to abolish its NLS (and to express a LexA-WT CDK10ΔNLS bait protein) and we verified that the interaction phenotypes with WT CycM (and other preys) were maintained. LexA-WT CycM, a strong transcriptional activator on its own (not shown), was discarded from the assay. 'Mut CycM' designates p.(Trp217X) CycM

Next, we examined whether these heterodimers exhibit a preserved protein kinase activity, using an optimized peptide substrate and an *in vitro* luminescent assay

described recently (Robert et al., 2020). As previously observed, WT CDK10/WT CycM exerted a robust kinase activity that was almost totally inhibited by NVP-2, a selective CDK9/CDK10 small-molecule inhibitor. KD CDK10/WT CycM produced a background activity, insensitive to NVP-2. p.(Trp291Alafs*18) CDK10/WT CycM produced a very reduced kinase activity (<20% of that of the WT kinase), which was neither significantly inhibited by NVP-2 nor significantly different from that of the dead kinase mutant. WT CDK10/p.(Trp217X) CycM produced a residual kinase activity (40% of that of the WT kinase), which was almost totally abolished by NVP-2 (Figure 2b).

The preserved formation of heterodimers between the CDK10 and CycM mutant forms and their WT partners, when overexpressed in insect cells, prompted us to examine whether these mutants are still able to interact with other proteins. To this end, we performed yeast two-hybrid mating assays which are ideally suited to determine interaction profiles of missense or truncated variants (Colas, 2020). The interactions between CDK10 and ETS2 and between CDK10 and CycM were previously shown to produce strong yeast two-hybrid interaction phenotypes (Guen et al., 2013; Kasten & Giordano, 2001), which we observed here again (Figure 3). We also observed a strong interaction phenotype between WT CycM and SALL1, a transcriptional repressor that was previously shown to physically interact with CycM (Unger et al., 2008) and whose mutations cause Townes-Brocks syndrome (Kohlhase, Wischermann, Reichenbach, Froster, & Engel, 1998). Interestingly, an interaction phenotype was also observed between SALL1 and WT CDK10, suggesting the existence of a trimeric complex with CycM. p.(Trp291Alafs*18) CDK10 did not retain any of the interaction phenotypes produced by WT CDK10, including that

with WT CycM, despite the physical interaction detected between the recombinant proteins overexpressed in insect cells. On the other hand, p.(Trp217X) CycM retained a residual, weak interaction phenotype with WT CDK10, observed in both two-hybrid orientations (i.e. when expressed as bait or as prey). However, it produced no detectable phenotype with SALL1 (Figure 3).

3.3 | Protein expression and stability in human cells

The fact that a robust formation of CDK10/CycM heterodimers could not be detected in yeast with either mutant is not congruent with the co-purifications observed from insect cells, and it points to low levels of expression, likely due to protein instability. To confirm this hypothesis, we compared the protein abundance of WT CDK10 and p.(Trp291Alafs*18) CDK10 on the one hand, WT CycM and p.(Trp217X) CycM on the other hand, upon transient expression in the human telomerase reverse transcriptase retinal pigmented epithelial (hTERT RPE-1) cellular model, which we previously used to unveil the role of CDK10/CycM in the regulation of ciliogenesis (Guen et al., 2016). While the expression level of Myc-tagged WT CDK10 was robust, that of Myc-tagged p.(Trp291Alafs*18) CDK10 was barely detectable, giving rise to a slight signal that added up to a co-migrating non-specific signal (Figure 4a). Strikingly, it was much enhanced in cells treated with MG132, a potent proteasome inhibitor that did not impact the expression level of WT CDK10 (Figure 4a). Although much lower than that of

WT CycM, the expression level of p.(Trp217X) CycM was readily detected and was augmented in response to MG132 (Figure 4b). These results show that p.(Trp291Alafs*18) CDK10 and p.(Trp217X) CycM are subjected to a massive and a partial degradation by the proteasome, respectively, which offers a likely explanation for the absent or weak interaction phenotypes observed in yeast two-hybrid assays, and which is in line with the reduced level of expression of p.(Trp291Alafs*18) CDK10 observed in insect cells.

4 | DISCUSSION

As predicted by our structural model, the p.(Trp291Alafs*18) CDK10 and p.(Trp217X) CycM pathogenic variants retain their ability to heterodimerize with WT CycM and WT CDK10, respectively. However, whereas the WT CDK10/p.(Trp217X) CycM heterodimer retains significant residual kinase activity *in vitro*, the p.(Trp291Alafs*18) CDK10/ WT CycM heterodimer is inactive, which points to a participation of the C-terminal region of CDK10 in the enzymatic process. In addition to the well-described conformational ordering of the T-loop triggered by the phosphorylation of a key threonine residue (here, T196; Brown, Noble, Endicott, & Johnson, 1999), an additional structural requirement for CDK activation has been described for the CDK12/CycK (Bosken et al., 2014) and CDK13/CycK (Greifenberg et al., 2016) kinases. In both CDKs, a C-terminal extension folds onto the N- and C-terminal lobes of the kinase and contacts the ATP ribose. The C-terminal region of CDK10 (residues 330-360, not covered by the Phyre2 model and absent
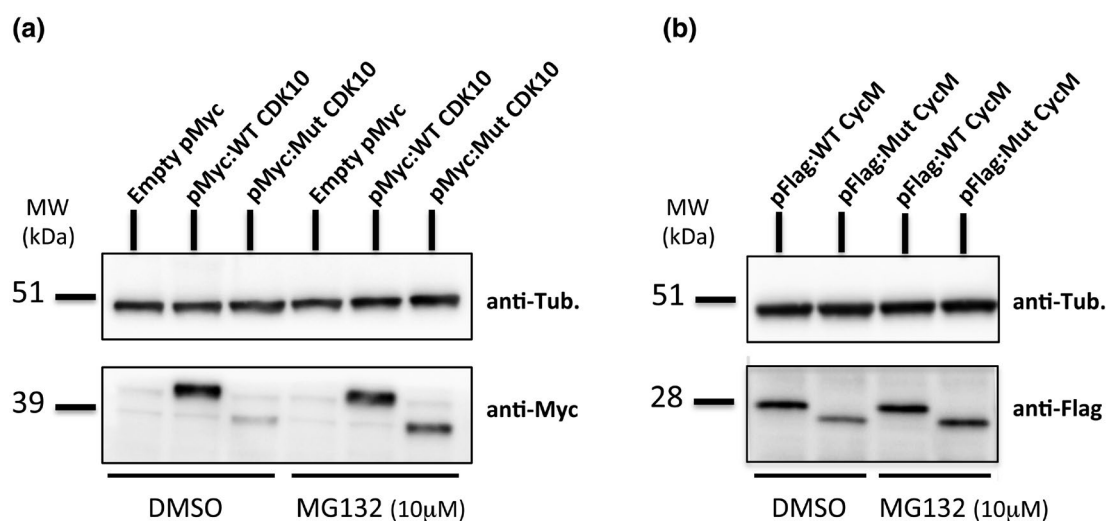

FIGURE 4 Expression and stability in human cells. Myc-tagged WT and p.(Trp291Alafs*18) CDK10 (a), Flag-tagged WT and p.(Trp217X) CycM (b) were expressed in hTERT-RPE1 human cells in the absence (DMSO) or presence of 10 μM MG132, and their level of expression was determined by Western blotting using an anti-Myc or an anti-Flag antibody (lower panels). Upper panels: loading controls using an anti-tubulin antibody. 'Mut CDK10' and 'Mut CycM' designate p.(Trp291Alafs18*) CDK10 and p.(Trp217X) CycM, respectively

from the p.(Trp291Alafs*18) CDK10 mutant) could similarly bring an essential contribution to the enzymatic activity. In the p.(Trp217X) CycM mutant, the two missing helices (α4* and α5*) might destabilize the second cyclin box and impact the position of the α3 and α5 helices in the first cyclin box, which is directly involved in the interface with CDK10. It might also impact the loop located at the C-terminus of α3 which contacts the essential arginine of the PISSLRE CDK10 motif and participates in the structuration of the T-loop. Whatever the structural perturbations caused by the absence of the last 32 residues, they still allow for a significant residual kinase activity.

The results of the yeast two-hybrid interaction profiling, the reduced levels of expression observed in insect and human cells, and the enhanced levels of expression in response to proteasome inhibition strongly suggest that these two pathogenic protein variants are absent or present at very low levels in patients. If the hypothesis of a mislocalized CDK10/CycM kinase activity in the patient expressing the p.(Trp291Alafs*18) CDK10 variant can be excluded (Guen et al., 2018), we cannot rule out the existence of low levels of mislocalized, catalytically inactive truncated CDK10 that might partially titrate CycM and possibly other interaction partners, away from the nucleus. Added to the loss of CDK10/CycM kinase activity, such putative molecular perturbations could account for the more severe clinical condition of the patient compared with the nine members of the cohort who present a total loss of *CDK10* expression. The partial stability of the p.(Trp217X) CycM variant and the partial kinase activity displayed by the WT CDK10/p. (Trp217X) CycM heterodimer suggests that the patients might retain a reduced CDK10/CycM kinase activity which, in view of their phenotypic presentations, would be anyhow insufficient to fulfil the essential functions of the kinase during development. The fact that no male STAR patient has been reported so far strongly suggests that total loss-of-function of *CCNQ* is lethal in males. However, quite intriguingly, the maternal grandfather displayed large distinctive ears similar to his affected daughter and grand daughters, and syndactyly of fingers and toes (Boczek et al., 2017). Residual activity of the WT CDK10/p.(Trp217X) CycM kinase might contribute to the viability of mosaicism of this CycM variant in males.

The toolbox deployed in this study (structural model, insect cell expression system, *in vitro* kinase assay, yeast two-hybrid interaction profiling, human cell expression system) will enable the functional characterization of further manmade or naturally occurring *CDK10* and *CCNQ* missense or truncating mutations that might preserve the expression of the proteins and cause selective losses of function (Colas, 2020). Until the crystal structure is solved, this will shed light on the structural determinants of the formation of the CDK10/CycM heterodimer, of the active kinase, and of the interactions with additional protein partners. This will also help to uncover novel functions of CDK10/CycM by linking functional characterization data to patient phenotypes.

CONFLICT OF INTERESTS
The authors declare that there are no conflict of interests.

AUTHOR CONTRIBUTIONS
The final manuscript has been read and approved by all authors. T.R. performed recombinant protein expression in insect cells and *in vitro* kinase assays. A.C.D.B. built the structural model, drew structural hypothesis from the experimental results, and wrote the structural sections of the manuscript. P.C. constructed the expression plasmids, performed the protein pull-down experiments, the yeast two-hybrid assays, the human cell experiments and wrote the manuscript.

DATA AVAILABILITY STATEMENT
The data that support the findings of this study are available from the corresponding author upon reasonable request.

ORCID
Pierre Colas https://orcid.org/0000-0001-7436-3718

REFERENCES
Boczek, N. J., Kruisselbrink, T., Cousin, M. A., Blackburn, P. R., Klee, E. W., Gavrilova, R. H., & Lanpher, B. C. (2017). Multigenerational pedigree with STAR syndrome: A novel FAM58A variant and expansion of the phenotype. *American Journal of Medical Genetics Part A*, *173*(5), 1328–1333. https://doi.org/10.1002/ajmg.a.38113

Bosken, C. A., Farnung, L., Hintermair, C., Merzel Schachter, M., Vogel-Bachmayr, K., Blazek, D., Anand, K., Fisher, R. P., Eick, D., & Geyer, M. (2014). The structure and substrate specificity of human Cdk12/Cyclin K. *Nature Communications*, *5*, 3505. https://doi.org/10.1038/ncomms4505

Brown, N. R., Noble, M. E., Endicott, J. A., & Johnson, L. N. (1999). The structural basis for specificity of substrate and recruitment peptides for cyclin-dependent kinases. *Nature Cell Biology*, *1*(7), 438–443. https://doi.org/10.1038/15674

Colas, P. (2020). Cyclin-dependent kinases and rare developmental disorders. *Orphanet Journal of Rare Diseases*, *15*(1), 203. https://doi.org/10.1186/s13023-020-01472-y

Finley, R. L. Jr, & Brent, R. (1994). Interaction mating reveals binary and ternary connections between Drosophila cell cycle regulators. *Proceedings of the National Academy of Sciences of*

the United States of America, *91*(26), 12980–12984. https://doi.org/10.1073/pnas.91.26.12980

Gietz, R. D., & Woods, R. A. (2006). Yeast transformation by the LiAc/SS carrier DNA/PEG method. *Methods in Molecular Biology*, *313*, 107–120. https://doi.org/10.1385/1-59259-958-3:107

Greifenberg, A. K., Honig, D., Pilarova, K., Duster, R., Bartholomeeusen, K., Bosken, C. A., Anand, K., Blazek, D., & Geyer, M. (2016). Structural and functional analysis of the Cdk13/cyclin K complex. *Cell Reports*, *14*(2), 320–331. https://doi.org/10.1016/j.celrep.2015.12.025

Guen, V. J., Edvardson, S., Fraenkel, N. D., Fattal-Valevski, A., Jalas, C., Anteby, I., Shaag, A., Dor, T., Gillis, D., Kerem, E., Lees, J. A., Colas, P., & Elpeleg, O. (2018). A homozygous deleterious CDK10 mutation in a patient with agenesis of corpus callosum, retinopathy, and deafness. *American Journal of Medical Genetics Part A*, *176*(1), 92–98. https://doi.org/10.1002/ajmg.a.38506

Guen, V. J., Gamble, C., Flajolet, M., Unger, S., Thollet, A., Ferandin, Y., Superti-Furga, A., Cohen, P. A., Meijer, L., & Colas, P. (2013). CDK10/cyclin M is a protein kinase that controls ETS2 degradation and is deficient in STAR syndrome. *Proceedings of the National Academy of Sciences of the United States of America*, *110*(48), 19525–19530. https://doi.org/10.1073/pnas.1306814110

Guen, V. J., Gamble, C., Lees, J. A., & Colas, P. (2017). The awakening of the CDK10/Cyclin M protein kinase. *Oncotarget*, *8*(30), 50174–50186. https://doi.org/10.18632/oncotarget.15024

Guen, V. J., Gamble, C., Perez, D. E., Bourassa, S., Zappel, H., Gartner, J., Lees, J. A., & Colas, P. (2016). STAR syndrome-associated CDK10/Cyclin M regulates actin network architecture and ciliogenesis. *Cell Cycle*, *15*(5), 678–688. https://doi.org/10.1080/15384101.2016.1147632

Kasten, M., & Giordano, A. (2001). Cdk10, a Cdc2-related kinase, associates with the Ets2 transcription factor and modulates its transactivation activity. *Oncogene*, *20*(15), 1832–1838. https://doi.org/10.1038/sj.onc.1204295

Kelley, L. A., Mezulis, S., Yates, C. M., Wass, M. N., & Sternberg, M. J. E. (2015). The Phyre2 web portal for protein modeling, prediction and analysis. *Nature Protocols*, *10*(6), 845–858. https://doi.org/10.1038/nprot.2015.053

Kohlhase, J., Wischermann, A., Reichenbach, H., Froster, U., & Engel, W. (1998). Mutations in the SALL1 putative transcription factor gene cause Townes-Brocks syndrome. *Nature Genetics*, *18*(1), 81–83. https://doi.org/10.1038/ng0198-81

Kurosaki, T., Popp, M. W., & Maquat, L. E. (2019). Quality and quantity control of gene expression by nonsense-mediated mRNA decay. *Nature Reviews Molecular Cell Biology*, *20*(7), 406–420. https://doi.org/10.1038/s41580-019-0126-2

Lauberth, S. M., & Rauchman, M. (2006). A conserved 12-amino acid motif in Sall1 recruits the nucleosome remodeling and deacetylase corepressor complex. *Journal of Biological Chemistry*, *281*(33), 23922–23931. https://doi.org/10.1074/jbc.M513461200

Robert, T., Johnson, J. L., Guichaoua, R., Yaron, T. M., Bach, S., Cantley, L. C., & Colas, P. (2020). Development of a CDK10/CycM in vitro Kinase Screening Assay and Identification of First Small-Molecule Inhibitors. *Frontiers in Chemistry*, *8*, 147. https://doi.org/10.3389/fchem.2020.00147

Sergere, J. C., Thuret, J. Y., Le Roux, G., Carosella, E. D., & Leteurtre, F. (2000). Human CDK10 gene isoforms. *Biochemical and Biophysical Research Communications*, *276*(1), 271–277. https://doi.org/10.1006/bbrc.2000.3395

Unger, S., Bohm, D., Kaiser, F. J., Kaulfuss, S., Borozdin, W., Buiting, K., Burfeind, P., Bohm, J., Barrionuevo, F., Craig, A., Borowski, K., Keppler-Noreuil, K., Schmitt-Mechelke, T., Steiner, B., Bartholdi, D., Lemke, J., Mortier, G., Sandford, R., Zabel, B., ... Kohlhase, J. (2008). Mutations in the cyclin family member FAM58A cause an X-linked dominant disorder characterized by syndactyly, telecanthus and anogenital and renal malformations. *Nature Genetics*, *40*(3), 287–289. https://doi.org/10.1038/ng.86

Vangone, A., Spinelli, R., Scarano, V., Cavallo, L., & Oliva, R. (2011). COCOMAPS: A web application to analyze and visualize contacts at the interface of biomolecular complexes. *Bioinformatics*, *27*(20), 2915–2916. https://doi.org/10.1093/bioinformatics/btr484

Windpassinger, C., Piard, J., Bonnard, C., Alfadhel, M., Lim, S., Bisteau, X., Blouin, S., Ali, N. B., Ng, A. Y. J., Lu, H., Tohari, S., Talib, S. Z. A., van Hul, N., Caldez, M. J., Van Maldergem, L., Yigit, G., Kayserli, H., Youssef, S. A., Coppola, V., ... Kaldis, P. (2017). CDK10 mutations in humans and mice cause severe growth retardation, spine malformations, and developmental delays. *The American Journal of Human Genetics*, *101*(3), 391–403. https://doi.org/10.1016/j.ajhg.2017.08.003